

# Continuous and Simultaneous Measurement of Micro Multiphase Flow Using confocal Micro-Particle Image Velocimetry (Micro-PIV)

Marie Oshima<sup>1\*</sup>, Masamichi Oishi<sup>2</sup>

\* Corresponding author: Tel.: +81 (0)3 5452 6205; Fax: +81 (0)3 5452 6205; Email: marie@iis.u-tokyo.ac.jp  
1: Interfaculty Initiative in Information Studies/Institute of Industrial Science,  
The University of Tokyo, Japan  
2: Institute of Industrial Science, The University of Tokyo, Japan

**Abstract** The objective of the paper is to present a “Multicolor Confocal Micro Particle Image Velocimetry (Micro-PIV)” technique to visualize and measure dynamic behavior of each phase of micro multiphase flow separately and simultaneously. The technique is applied to two types of micro two-phase flow. The first case is to investigate a mechanism of micro droplet formation at a micro T-shaped junction. The measurement data are compared to the numerical simulation using the CIP method. The second case is to investigate the tank-tread motion of red blood cell induced by the surrounding plasma flow.

**Keywords:** Confocal Micro-PIV, Micro Droplet, CIP Method

## 1. Introduction

A microfluidic device can have various functions such as sensing or mixing on a small chip in a size from a few millimeters to a few centimeters (Auroux, et al, 2002). In general, the device usually deals with more than two different materials, i.e., a “multiphase flow”, for example, solid-liquid multiphase flow for blood analysis (Shevkoplyas, et al 2005) or liquid-liquid multiphase flow for micro droplets used in a drug delivery system. In order to clarify the phenomenon of micro multiphase flow inside these devices, it is necessary to measure the flow field or movement of each phase simultaneously.

For visualization and measurement of multiphase flows in a microchannel, a confocal micro-PIV technique is a powerful tool such that it can non-invasively measure the velocity distribution of a microflow with high-resolution. Since one of its advantages is a very thin measurement depth (Kim, et al, 2003, Kinoshita, et al, 2006), the three-dimensional velocity field can be obtained by calculating an out of plane velocity from the continuity equation.

However, it is important to measure the interaction between two phases simultaneously. The objective of the paper is to give an overview of the multicolor confocal micro-PIV technique, which has been developed by the authors (Oishi, et al, 2011, 2012). In order to show the capability of the system, the paper presents two types of applications. The first one is to observe the dynamic behavior in generation of micro droplets in a microchannel with a T-junction. The second one is to measure the tank tread motion of red blood cells.

## 2. Multicolor confocal micro-PIV system

The multicolor confocal micro-PIV system is developed based on a conventional confocal micro-PIV system (Kinoshita, et al, 2006). To measure two different phases simultaneously and separately, the system has an extra set of laser and camera in addition to one set in the conventional system with a multi-wavelength separation unit. Two different types of illumination laser beams are combined using a dichroic mirror in a laser combiner. The lasers

illuminate the target, and scattered lights from the target return through a confocal scanner. Multi-wavelength emitted lights are then separated at the separation unit and are recorded by two high-speed cameras. Details of the multicolor confocal micro-PIV system can be found in Oishi, et al (2011)

However, the range of velocities that can be measured by the confocal micro-PIV has a limit, which is determined by the rotational speed of the confocal scanner. One of applications in the paper focuses on the tank-tread motion of red blood cells. Since the tank-tread motion of red blood cells is induced by the velocity of their surrounding plasma larger than that of the confocal scanner, a translational stage has been added to the multicolor confocal micro-PIV system (Oishi, et al, 2012). The targeted microchannel is moved in the direction opposite to the flow in the channel by a motorized stage to keep the measurement target in the field of view as shown in Fig.1. The proposed technique can measure flows not only faster but also for longer period of time than the previous confocal micro-PIV system.

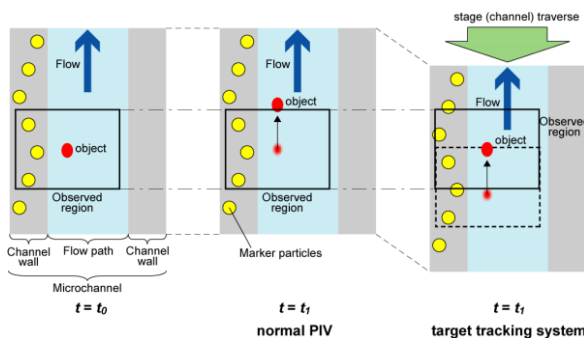


Fig.1. Schematic illustration of tracking system (Oishi, et al, *Meas. Sci. Tech.*, 2012)

The motorized stage should move at constant velocity with high precision and little vibration. A stepping motorized stage with an air bearing (VMDA-100, PMT Corp., Japan) was chosen for this purpose. The 100x oil-immersion objective lens (PL APO CS 100x/1.4-1.25 HCX, Leica Microsystems, Germany) provide the sufficient spatial resolution of 0.116  $\mu\text{m}/\text{pixel}$  in plane and the confocal depth of 0.58  $\mu\text{m}$  with  $\phi$  0.2  $\mu\text{m}$  tracer particle.

The absolute flow velocity is obtained by subtracting the velocity of the tracer particles from that of the marker particles, which are imbedded in a sub-channel adjacent to the main channel.

### 3. Measurement for Droplet Formation

The size of a micro droplet is determined in the process of its formation, which depends on the size of channel or the either velocity of continuous or disperse flow. The micro droplet can be categorized depending on the Capillary number  $Ca$  defined by a ratio of the shear force  $F_s$  to the interfacial tension  $F_i$  as follows:

$$Ca = \frac{F_s}{F_i} \equiv \frac{U_c \mu_c}{\gamma} \quad (1)$$

where  $U_c$  is the velocity of the continuous flow,  $\mu_c$  is the viscosity, and  $\gamma$  is the interfacial tension.

As  $Ca$  increases, the size of micro droplet becomes smaller from a tank-like shape to a droplet-like shape (Garstecki, et al, 2006). In order to elucidate its mechanism, the micro confocal scanner without the translational stage is applied to measure the velocity fields of both continuous and dispersed flows in a T-junction microchannel. Since it is quite difficult to measure forces such as the shear force, a numerical simulation study is also conducted.

#### 3.1 Numerical Method

In the formation of a droplet, the surface tracking method is difficult for a problem with large deformation and changes in the topology. Thus, in this study, the CIP (Constrained Interpolation Profile) method (Yabe, et al, 1993, Xiao, et al 1996) is applied using the finite volume method (Nakamura, T. et al, 2001.). The CIP method uses a cube function for interpolation so that the advective term can be discretized with less dispersion errors. In order to capture the surface with high accuracy, the particle method is combined with the CIP method.

### 3.2 Experimental and Numerical Conditions

The simulation is performed to the flow in the T-junction microchannel as shown in Fig.2. The confocal micro PIV without the translational stage is also conducted to the

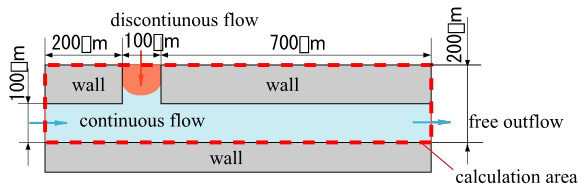
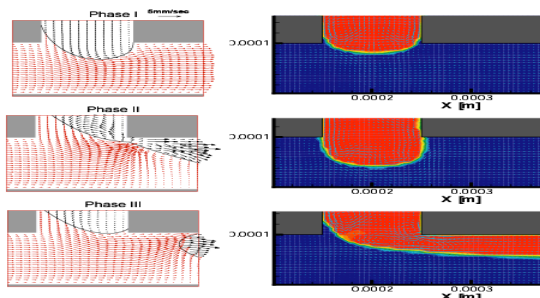


Fig. 2. The T-junction microchannel

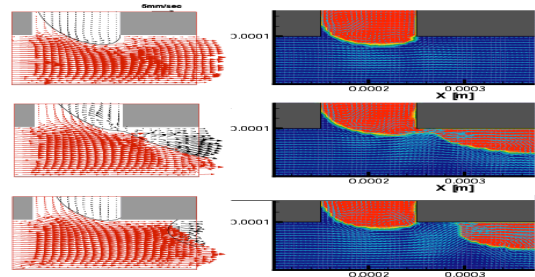
same flow.

The continuous phase consists of silicon oil with a density of 0.984 g/cc and the viscosity 44.15 mPa.s while the dispersed phase consists of glycerol solution with a density of 1.162 g/cc and viscosity of 10.58 mPa.s. The simulations are performed for two cases,  $Ca = 1.66 \times 10^{-3}$  as a tank-like shape and  $Ca = 1.68 \times 10^{-2}$  as a droplet-like shape. The interfacial tension is 11.7 mN/m and the averaged velocity of the dispersed flow is 0.22 mm/sec. The averaged velocity of the continuous flow for the first case (Case 1) is 0.44 mm/sec while that for the second case (Case 2) is 4.44 mm/sec.

The flow patterns of both cases are obtained by the PIV measurement and the simulation described in Figs.3 a) and b). The figures on the left hand side in Fig.3 are results from the PIV measurement while the ones on the right are from the CIP simulation. s



a)  $Ca = 1.66 \times 10^{-3}$



b)  $Ca = 1.68 \times 10^{-2}$

Fig. 3. Flow patterns of continuous and dispersed flows

If Ca number is small, the shear force from the continuous flow becomes smaller, in which a tank shaped droplet tends to be created. This process is called squeezing. On the other hand, as Ca number becomes larger, the shape of droplet becomes a small round droplet. This is called dripping. These tendencies are observed in both experimental and simulations results. The simulation in this paper is conducted in the 2-dimension. However, it will be extended to the 3-dimensional simulation and some of results will be presented in the conference.

## 4. Measurement of Tank-Treading Motion of Red Blood Cells

In order to initiate the tank-tread motion of the red blood cells, the shear force needs to be larger than 0.3Pa. The conventional confocal micro PIV has a limit in the velocity of 0.70 mm/s, which corresponds to a force less than 0.3 Pa. Thus, the translational confocal micro PIV technique is employed to overcome the drawback of the conventional one with longer observation time.

### 4.1 Experimental Conditions

Figure 4 shows the geometry of the target microchannel. The field of view of the measurement slice is  $92.8 \times 69.6 \mu\text{m}$  at channel center height. The flow shear stress is adjusted to 0 – 2.9 Pa by controlling the flow rate at  $2.5 \mu\text{l/h}$  with physiologically-controlled surrounding fluid. Under the conditions above, the shear rate becomes  $0 \sim 152.4 \text{ s}^{-1}$ , and this value satisfies the physiological condition with

the possibility of tank tread motion. The translational velocity of the moving stage is set to 0.7 mm/s to cover the whole velocity range from zero to the maximum flow velocity of 1.25 mm/s. The carboxylate-modified yellow-green fluorescent tracer particle 0.2  $\mu\text{m}$  in diameter (F8813, Invitrogen Molecular Probes, USA) is attached electrically to the surface of RBCs to visualize the deformation and movement of the membrane of RBC.

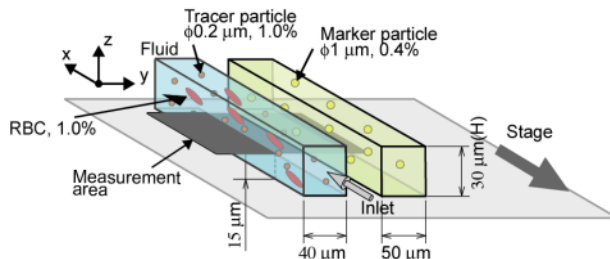
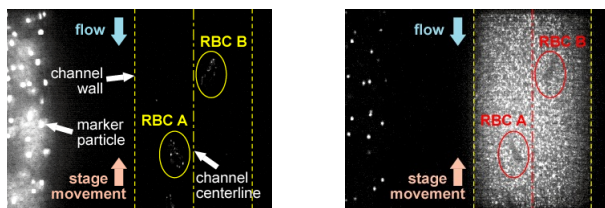


Fig. 4. Measurement target microchannel.

#### 4.2 Results

Figure 5 shows PIV images of RBCs and the surrounding flow separated by different wavelengths. The channels run in the vertical direction of the images, and the RBC suspended fluid flows downward. We succeeded in recording continuous images of RBC A for 0.1 s. The present system can measure 2.56 times longer continuous measurement compared with the conventional system.



a) Images of RBC

b) Images for surrounding flow

Fig.5. PIV images at  $t = 0.06$

Figure 6 shows the relative velocity distribution of the RBC membrane and the surrounding fluid overlapped at  $t = 0.04$  sec. The relative velocities of these two phases are calculated by subtracting the translational velocity of the center of gravity of the RBC in order to investigate the interaction. Since the absolute velocity of RBC A was 1.15 mm/s, the present system succeeded to measure the faster flow and overcome the limitation of the

conventional system. The vector map shows only the region around RBC A, and the channel centerline is indicated as dashed line on the right side of the RBC. The velocities of the tracer particle attached on the RBC membrane are indicated by red circles.

The flow around the RBC is distorted in the same direction as the rotational direction of the RBC membrane. The velocities on RBC membrane also show the same magnitudes as the adjacent flow velocities. This indicates there is strong interaction between RBC motion and surrounding flow. Moreover, the particle velocity on the RBC membrane varies depending on their position. The membrane velocity on the channel centerline side of RBCs is larger than that of channel sidewall side. It suggests that the RBC membrane may have stretch and show hyper elastic material properties depending on the shear stress induced by the surrounding flow. The membrane curvature on channel centerline side of RBCs is larger than that of channel sidewall side. We consider that this difference in the membrane curvature enhances the difference in the lateral velocity component, and results in the one reason of axial migration.

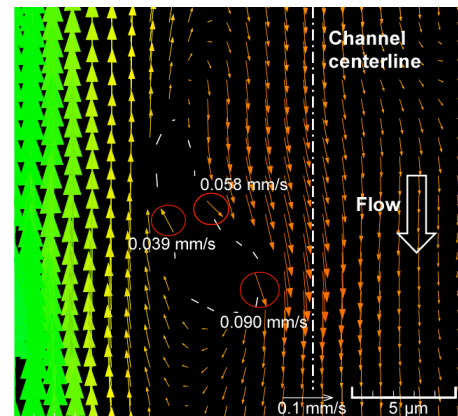


Fig. 6. Distribution of velocity vectors

## 5. Conclusions

The paper presented two cases of measurements using the confocal micro PIV technique. The first case shows the measurement of both continuous and dispersed flow in the T-junction microchannel using the confocal micro PIV without the translational

stage in order to investigate the mechanism of droplet formation. A simulation study is also performed to the same flow. Since the simulation is conducted in 2-simensions, the shear force in the continuous flow tends to be underestimated. Thus, the flow tends to become sheath flow. The simulation will be extended to the three dimensional calculation in the future.

The second case is to measure the tank-tread motion of red blood cells. Since the measurable velocity is limited by the rotational speed of the confocal scanner, we have developed a target-tracking confocal micro-PIV system that can measure faster flows than the conventional system with a motorized stage. The movement of the RBCs and the velocity distribution of the surrounding flow are successfully measured simultaneously using the present system. The proposed system enables continuous observation of moving RBCs over a distance 2.5 times longer than that of the conventional system. It can also measure higher absolute velocities than the conventional system does.

As a result, the tank-tread motion of RBCs and the corresponding movement of the surrounding flow structure are measured simultaneously and quantitatively. The rotational direction of the tank-tread motion corresponds to the shear stress gradient of the surrounding flow. The tank-tread motion also affects the surrounding flow structure. The relationship between the tank-tread frequency and the shear rate will be investigated quantitatively.

## Acknowledgements

This work was supported in part by the Ministry of Education, Culture, Sports, Science, and Technology through Grants-in-Aid for Young Scientists (B), nos. 17760134 and 21760121. This work was also funded by The Asahi Glass Foundation, 2010, No.58.

## References

Auroux, P. A., Iossifidis, D., Reyes, D. R. and Manz, A. 2002 *Anal. Chem.* **74** 2637-2652.  
Fischer, T. M., Stohr-Liesen, M. and Schmid

Schonbein, H. 1978 *Science*, **202** 894-906.

Garstecki, et al, *Lab on a Chip*, 2006, **6** 437-446.

Kim, H. J., Kihm, K. D. and Allen, J. S. 2003 *Int. J. Heat Mass Transfer* **46** 3967-3974.

Kinoshita, H., Kaneda, S., Fujii, T., and Oshima, M., 2006 *Lab on a Chip*, **7** 338-346.

Nakamura, T. et al, *J. Comput. Phys.* 2001, **174**, 171-207,

Oishi, M., Kinoshita, H., Fujii, T. and Oshima, M. 2011 *Meas. Sci. Tech.*, **22**, 105401-105414.

Oishi, M., Utsubo, K., Kinoshita, H., Fujii, T., and Oshima, M., 2012 *Meas. Sci. Tech.*, **23**, 35301-35219.

Shevkoplyas, S. S., Yoshida, T, Munn. L. L, and Bitensky, M. W. 2005 *Anal. Chem.* **33** 933-937.

Tice, J. D., Song, H., Lyon A. D. and Ismagilov, R. F. 2003 *Langmuir* **19** 9127-9133.

Xiao, F., Yabe, T., Ito, T., *Comp. Phys. Comm.*, 1996, **93** 1-12.

Yabe, T. Xiao, F., *J Phys. Soc. Japan*, 1993, **62** 2537-2540.